JCTC Journal of Chemical Theory and Computation

Article

pubs.acs.org/JCTC

Magnetic Couplings in the Chemical Shift of Paramagnetic NMR

Juha Vaara,* Syed Awais Rouf, and Jiří Mareš

NMR Research Group, University of Oulu, P.O. Box 3000, FIN-90014 Oulu, Finland

Supporting Information

ABSTRACT: We apply the Kurland–McGarvey (*J. Magn. Reson.* **1970**, *2*, 286) theory for the NMR shielding of paramagnetic molecules, particularly its special case limited to the ground-state multiplet characterized by zero-field splitting (ZFS) interaction of the form $\boldsymbol{S}\cdot\boldsymbol{D}\cdot\boldsymbol{S}$. The correct formulation for this problem was recently presented by Soncini and Van den Heuvel (*J. Chem. Phys.* **2013**, *138*, 054113). With the effective electron spin quantum number S, the theory involves $2S+1$ states, of which all but one are low-lying excited states, between which magnetic couplings take place by Zeeman and hyperfine interactions. We investigate these couplings as a function of temperature, focusing on both the high- and low-temperature behaviors. As has been seen in work by others, the full treatment of magnetic couplings is crucial for a realistic description of the temperature behavior of NMR shielding up to normal measurement temperatures. At high temperatures, depending on the magnitude of ZFS, the effect of magnetic couplings diminishes, and the Zeeman and hyperfine interactions become effectively averaged in the thermally occupied states of the multiplet. At still higher temperatures, the ZFS may be omitted altogether, and the shielding properties may be evaluated using a doublet-like formula, with all the $2S+1$ states becoming effectively degenerate at the limit of vanishing magnetic field. We demonstrate these features using first-principles calculations of Ni(II), Co(II), Cr(II), and Cr(III) complexes, which have ZFS of different sizes and signs. A non-monotonic inverse temperature dependence of the hyperfine shift is predicted for axially symmetric integer-spin systems with a positive D parameter of ZFS. This is due to the magnetic coupling terms that are proportional to kT at low temperatures, canceling the Curie-type $1/kT$ prefactor of the hyperfine shielding in this case.

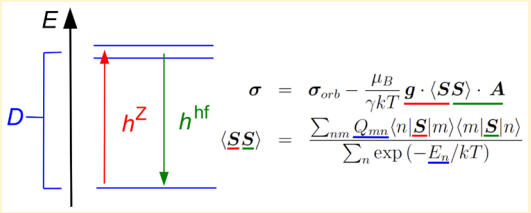

1. INTRODUCTION

Nuclear magnetic resonance (NMR) of electronically open-shell, paramagnetic molecules (pNMR) is gaining importance in biomolecular and materials science.[1−4] Electronic structure methods for determining the central NMR parameter, the shielding tensor $\boldsymbol{\sigma}$, and the associated chemical shift δ can aid in the prediction, interpretation, and assignment of NMR spectra.[5] In open-shell systems, $\boldsymbol{\sigma}$ needs to be calculated in a manifold of thermally populated states, rendering it a more challenging task than in the case of conventional NMR of diamagnetic molecules with non-degenerate ground state.[6] A seminal contribution to the field is that of Kurland and McGarvey,[7] who presented a density matrix theory of pNMR shielding, leading first to a general expression involving Zeeman interactions with the external magnetic field $\boldsymbol{B}_0$ and the hyperfine interaction with the nuclear spin $\boldsymbol{I}_K$ coupling the electronic ground-state wave function to excited states. Furthermore, ref 7 formulated the contact, dipolar, and pseudocontact chemical shift contributions, as well as the effects of zero-field splitting (ZFS), in terms of the electron paramagnetic resonance (EPR) parameters, the g-tensor ($\boldsymbol{g}$) parametrizing the Zeeman interaction, the hyperfine coupling (HFC) tensor $\boldsymbol{A}_K$, and the D parameter of the ZFS Hamiltonian of the form $\boldsymbol{S}\cdot\boldsymbol{D}\cdot\boldsymbol{S}$, where $\boldsymbol{S}$ is the effective electron spin and $\boldsymbol{D}$ is the ZFS tensor.[8] The topic of paramagnetic shielding has been treated in several recent studies.[9−17] Significant progress has been made particularly by Soncini and Van den Heuvel,[12,13] who derived a general formulation for pNMR shielding in systems with arbitrary degeneracy of the electronic state in terms of generalized EPR tensors. This framework covers cases with strong spin–orbit (SO) coupling and is open-ended with respect to including not only the ground-state multiplet of $2S+1$ states (with S the effective spin quantum number of the system) but also the contributions of excited multiplets.[12]

Most of the contemporary quantum-chemical work on pNMR shieldings is based on treating only the ground-state multiplet and formulating the shielding tensor with the help of the parameters of the standard EPR Hamiltonian involving the electronic Zeeman, HFC, and ZFS terms, the latter in the form $\boldsymbol{S}\cdot\boldsymbol{D}\cdot\boldsymbol{S}$ despite the fact that this form is valid only at the limit of weak SO coupling.[12] In ref 14, Soncini and Van den Heuvel (SVH) presented the correct formula for the hyperfine shielding tensor in this special case. Computational applications of the SVH formula have since then been published, e.g., in refs 16 and 18. It should be pointed out that the method of ref 12 does go beyond the $\boldsymbol{S}\cdot\boldsymbol{D}\cdot\boldsymbol{S}$ form of the ZFS Hamiltonian. Besides the formal advances, the involvement of relativistic electronic structure theory[11,12,15,17] and the application of *ab initio* electronic structure methods[12,17,18] have increased the potential of quantum-chemical approaches in the prediction and interpretation of pNMR shifts. In particular, ref 17 reported a multiconfigurational self-consistent field study of pNMR shielding in which no use was made of the EPR parameters.

Received: July 9, 2015
Published: August 25, 2015

DOI: 10.1021/acs.jctc.5b00656
J. Chem. Theory Comput. 2015, 11, 4840–4849

The Kurland–McGarvey theory,[7] as well as its special case limited to the zero-field-split ground multiplet, described by the EPR Hamiltonian parameters,[14] features states coupled by magnetic perturbation operators. It has been shown in refs 14 and 16 that the correct behavior of the chemical shifts of $S > 1/2$ systems as a function of temperature is only reproduced by including these couplings. In contrast, ref 10 proposed a formula for the pNMR shielding that differs from the SVH result by omitting the magnetic couplings.[14] The formula of ref 10 is obsolete by now, as it offers no computational advantage whatsoever as compared to the exact SVH equation. However, it serves as means of assessing the effect of these couplings. In contrast, neglecting ZFS altogether and using a doublet-like theory[9] with all the $2S+1$ states degenerate at the limit of vanishing $\boldsymbol{B}_0$ is a computationally attractive option, as one does not have to calculate $\boldsymbol{D}$. The ZFS tensor is a demanding molecular property to be reproduced accurately, particularly for the computationally expedient density functional theory (DFT) methods.[19,20]

In this paper we investigate computationally particularly the high- and low-temperature limiting behaviors of the pNMR shielding according to the SVH theory, which can be viewed as including both (1) thermal averaging of the Zeeman and HFC interactions in the states of the ground-state multiplet and (2) magnetic couplings between the non-degenerate states. Depending on the size of the ZFS interaction, at sufficiently high temperatures, the effects of magnetic couplings become numerically negligible, but thermal averaging of the zero-field-split levels remains important. By increasing the temperature further, the thermal occupations of all the states of the ground multiplet become practically equal, and ZFS may be omitted altogether, leading to computational savings. We demonstrate these basic features on the $S = 3/2$ Co(II) and Cr(III) complexes that have large and small D parameters of ZFS, respectively. Furthermore, we report calculations on the axial $S = 1$ metallocenes $NiCp_2$ (nickelocene) and $CrCp_2$ (chromocene), which feature D parameters of both opposite signs and different sizes. Reference 16 reported the temperature dependence of the NMR shieldings in $NiCp_2$ by using a numerical implementation of the SVH theory. This system was found[16] to feature a non-monotonic behavior of the Curie plot (as a function of the inverse temperature) of the shift, and we show here, by comparison with $CrCp_2$, that the appearance of this feature in the present axially symmetric integer-spin system is related to the sign of D, which determines whether the upper or the lower level of the triplet manifold is doubly degenerate. A chemical shift extremum results from the cancellation of the Curie-type $1/kT$ dependence of the hyperfine shift by the magnetic coupling terms, which are proportional to kT at low temperatures.

2. THEORETICAL BACKGROUND

Straightforward application of the Kurland–McGarvey theory for the pNMR shielding tensor, outlined in the Supporting Information (SI), leads to the following formula for the Cartesian $\epsilon\tau$ component of the pNMR shielding tensor of nucleus K:

$$\sigma_{K,\epsilon\tau} = \sigma^{\mathrm{orb}}_{K,\epsilon\tau} - \frac{\mu_B}{\gamma_K \hbar k T} \sum_{ab} g_{\epsilon a} \langle S_a S_b \rangle A_{K,b\tau} \tag{1}$$

$$\langle S_a S_b \rangle = \frac{\sum_{nm} Q_{nm} \langle n|S_a|m\rangle \langle m|S_b|n\rangle}{\sum_n \exp(-E_n/kT)} \tag{2}$$

where $\boldsymbol{\sigma}^K_{\mathrm{orb}}$ is the orbital shielding tensor, analogous to the Ramsey theory for closed-shell compounds.[21] In the second, hyperfine shielding term, γ_K is the gyromagnetic ratio of nucleus K, $\boldsymbol{g}$ is the g-tensor, and Q_{mn} is a symmetric matrix with the elements

$$Q_{nm} = \begin{cases} \exp(-E_n/kT) & E_n = E_m \\ -\dfrac{kT}{E_m - E_n}[\exp(-E_m/kT) - \exp(-E_n/kT)] & E_n \neq E_m \end{cases} \tag{3}$$

$\langle \boldsymbol{SS} \rangle$ is a dyadic resulting from the effective spin operators $\boldsymbol{S}$, evaluated with the $2S+1$ states $|n\rangle$ (with energies E_n) of the ground multiplet. $|n\rangle$ and E_n are respectively the eigenfunctions and eigenvalues of the ZFS Hamiltonian $\boldsymbol{S}\cdot\boldsymbol{D}\cdot\boldsymbol{S}$ only, evaluated at the limit of vanishing $\boldsymbol{B}_0$.

Equation 1 is equivalent to the SVH hyperfine shielding formula derived in ref 14. The present, compact form is used here, because its symmetry properties match those of the earlier formula of ref 10. In the latter context, an analysis scheme was introduced in terms of the physical contributions to $\boldsymbol{g}$ (ref 9) and $\boldsymbol{A}_K$ (ref 22). Here, $\boldsymbol{g}$ is broken into the isotropic free-electron g-factor (g_e) and the g-shift tensor arising from the SO interaction, and $\boldsymbol{A}_K$ into the nonrelativistic, isotropic Fermi contact and anisotropic spin-dipole HFC terms, as well as the leading SO corrections to $\boldsymbol{A}_K$. This results in altogether nine hyperfine terms up to $O(\alpha^4)$ (α is the fine-structure constant), listed in Table S1 in the SI. The terms contribute to the different tensorial ranks in $\boldsymbol{\sigma}_K$ as presented in the table. Specifically, this implies (in the $S > 1/2$ cases) that eight terms contribute to the isotropic (rank-0) shielding constant (and chemical shift δ), and all the nine terms are included in the anisotropic but symmetric (rank-2) part of $\boldsymbol{\sigma}_K$. The form of eq 1 is also convenient for the present discussion of the high-temperature limiting behavior of the SVH theory. Both of these aspects are addressed below.

3. COMPUTATIONS

We implemented[18] the SVH method in the form of eq 1, as well as two of its high-temperature forms discussed below, in connection with the analyses of refs 10 and 18 for the different physical contributions, and applied the methodology to example 3d-transition metal complexes. Two $S = 3/2$ complexes were investigated, where the ground multiplet consists of two Kramers doublets split by ZFS. These are the cobalt(II) pyrazolylborate (code HPYBCO in the Cambridge Structural Database[23]) studied experimentally by ^{1}H solution pNMR in ref 24 and computationally using the present method in ref 18, where the D parameter of ZFS was found at 112 cm^{-1} at the N-electron valence-state perturbation theory (NEVPT2) level[25] with the def2-TZVP basis set.[26] This system represents, hence, a case with a very large ZFS. On the other hand, a quinolyl-functionalized cyclopentadienyl Cr(III) complex was studied, which has a much smaller D parameter, below 3 cm^{-1} according to the present NEVPT2/def2-TZVP calculations. ^{1}H pNMR shifts for a series of such complexes were taken in the solution state in ref 27, and we presently carry out ^{1}H shift computations for the particular molecule 1 studied in that

DOI: 10.1021/acs.jctc.5b00656
J. Chem. Theory Comput. 2015, 11, 4840–4849

paper. These $S = 3/2$ systems are presently considered to investigate the high-temperature behavior of the chemical shifts.

The $S = 1$ metallocenes nickelocene ($NiCp_2$) and chromocene ($CrCp_2$) were also studied. The M(II) metallocenes have been subjected to earlier pNMR shielding calculations in several occasions.[10,16,28,29] These two particular systems are included here because they represent different signs of the D parameter: In $NiCp_2$, positive experimental values of D in the range 25.6−33.6 cm^{-1} (refs 30−33) have been obtained, whereas the present NEVPT2/def2-TZVP calculations result in the value 40 cm^{-1}. In this case, the ground multiplet consists of a non-degenerate ground state separated by D from the excited doubly degenerate state. The opposite situation prevails for the $CrCp_2$ system, for which $D = -15.1$ cm^{-1} from experiment[34] and $D = -10.1$ cm^{-1} from the present NEVPT2/def2-TZVP computations. Experimental ^{13}C and ^{1}H pNMR data for these two systems have been reported both in solution and in the solid state.[35−39] The purpose of studying these metallocenes is to compare the low-temperature behavior of the shifts in the opposite cases where either the upper ($NiCp_2$) or lower ($CrCp_2$) level of the ground multiplet is doubly degenerate.

Computationally optimized geometries were used for HPYBCO and the metallocenes (eclipsed geometry), obtained as described in refs 18 and 10, respectively. The quinolyl-functionalized cyclopentadienyl Cr(III) complex was optimized using the B3LYP functional[40] and the def2-TZVP basis set using the TURBOMOLE code.[41] The optimized coordinates are listed in Table S2. The systems are illustrated in Figure 1. The magnetic properties were calculated, in the case of $\boldsymbol{g}$, $\boldsymbol{A}$, and $\boldsymbol{D}$, with the ORCA 3.0.1 software[42,43] and, for $\boldsymbol{\sigma}_{orb}$, with the GAUSSIAN 09 software.[44] The results are averaged over all the experimentally equivalent nuclei.

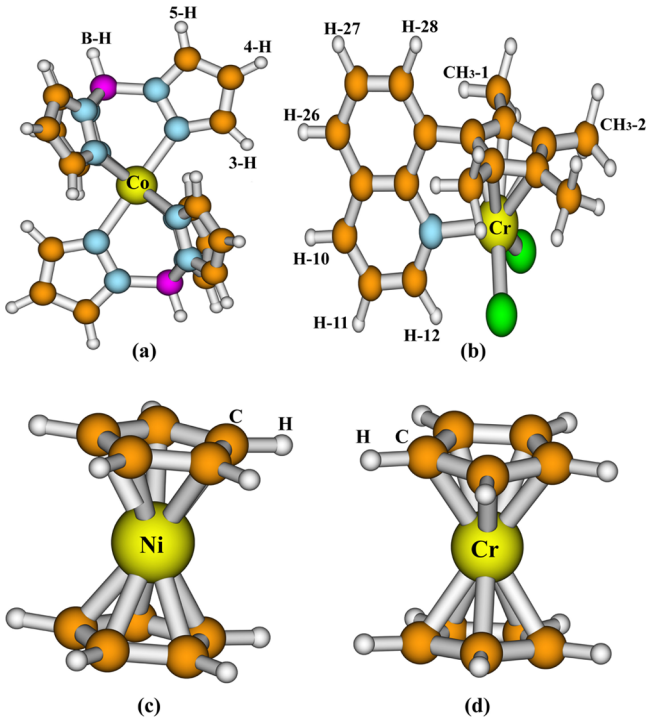

Figure 1. (a) Co(II) pyrazolylborate complex HPYBCO, (b) quinolyl-functionalized cyclopentadienyl Cr(III) complex, (c) nickelocene, and (d) chromocene. The groups of ^{1}H and ^{13}C nuclei, for which the pNMR shielding calculations are reported, are indicated.

In the case of the HPYBCO complex, NEVPT2, based on a CASSCF wave function correlating seven active electrons in the five metal 3d orbitals [CAS(7,5)], was used for $\boldsymbol{g}$ and $\boldsymbol{D}$. The Cr(III) complex was correspondingly treated by NEVPT2 based on a CAS(3,5) wave function. For these systems, a locally dense basis was used, consisting of the def2-TZVP set[26] applied for the metal ion and the directly bonded atoms, and the def2-SVP basis for the more distant atoms. The validity of this approach was verified in ref 18. For $\boldsymbol{A}$ and $\boldsymbol{\sigma}_{orb}$, DFT with the PBE0 exchange-correlation functional[45] and the full def2-TZVP basis on all atoms, were employed. For the metallocenes, we report the isotropic ^{13}C and ^{1}H chemical shifts, as well as, in the case of $NiCp_2$, the ^{13}C and ^{1}H shielding anisotropy $\Delta\sigma = \sigma_{\parallel} - \sigma_{\perp}$ with respect to the molecular axis, as a function of temperature. We report data with (1) $\boldsymbol{g}$ and $\boldsymbol{D}$ with CAS(8,5) for $NiCp_2$ and CAS(4,5) for $CrCp_2$, and (2) $\boldsymbol{g}$ and $\boldsymbol{D}$ with NEVPT2 based on CAS(8,5)/CAS(4,5), in all cases combined with $\boldsymbol{A}$ and $\boldsymbol{\sigma}_{orb}$ obtained with the PBE0 functional. The full def2-TZVP basis was used in all the metallocene calculations for all the atoms. The calculated properties of the ZFS and g-tensors of all the presently calculated complexes are listed in Table S3.

The present computational choices, particularly concerning the basis set and the DFT functional, follow the findings of ref 18 and represent a compromise. Specifically, the calculated $\boldsymbol{A}$-tensor is sensitive to the details of the functional used, and the deficiencies of any particular choice contribute to the deviation of the results from the experimental pNMR shifts. The focus of the present work is in the qualitative temperature dependence of the pNMR signals, however, a purpose for which the present compromise choices are adequate.

Besides causing ZFS and thereby entering the formal structure of the pNMR shielding model,[12,14] SO coupling also causes the deviation of $\boldsymbol{g}$ from the isotropic free-electron value as well as influences $\boldsymbol{A}$, as discussed above. Concerning the latter tensor, we include the SO corrections perturbationally, whereas the g- and D-tensors are obtained by a variational SO procedure. In addition, we presently omit all scalar relativistic effects from the calculated EPR tensors. This should constitute a fairly good approximation for the shieldings of light nuclei in 3d systems.

The diamagnetic chemical shift reference molecule was tetramethylsilane (TMS), with geometry optimized as described in ref 18 and with the shielding constants $\sigma(^{13}C) = 188.5$ ppm and $\sigma(^{1}H) = 31.8$ ppm at the PBE0/def2-TZVP level.

4. HIGH-TEMPERATURE LIMIT

Two characteristic physical features of the Kurland−McGarvey theory[7] (SI) as well as its special case limited to the zero-field split ground multiplet, according to the SVH theory (eq 1),[14] appear in the $\boldsymbol{Q}$ matrix of Kurland and McGarvey (eq 3). The diagonal blocks of this matrix correspond to groups of states $|n\rangle$ that are degenerate in the absence of an external magnetic field, and contain the Boltzmann factors $\exp(-E_n/kT)$ of these states. These diagonal blocks can be viewed to represent (*vide infra*) thermal averaging of the Zeeman and HFC interactions. On the other hand, the matrix components in the off-diagonal blocks of $\boldsymbol{Q}$ refer to two state indices, n and m, and represent magnetic couplings occurring via the Zeeman and HFC interactions between pairs of states that do not belong to the same degenerate manifold. These couplings arise because the eigenstates of either the magnetic field- or nuclear spin-free

DOI: 10.1021/acs.jctc.5b00656
J. Chem. Theory Comput. 2015, 11, 4840−4849

Hamiltonian H_0 in the general Kurland−McGarvey theory, or the ZFS Hamiltonian in the SVH theory, are generally not eigenstates of the Zeeman and HFC operators.

4.1. Magnetic Couplings. Normally NMR measurements are carried out at room temperature (ca. 298 K), which represents physically very different situations for systems with either a large or a small ZFS. One can define a dimensionless, effective temperature scale $T^* = kT/D$, according to which the present $S = 3/2$ HPYBCO system, with a large ZFS, is at $T^* = 1.8$ at room temperature, whereas the corresponding value for the present quinolyl-functionalized cyclopentadienyl Cr(III) complex, with $D \approx 3$ cm^{-1}, is about $T^* = 75$. In general, the high-temperature limit of a component in the off-diagonal (magnetic-coupling) block of $\mathbf{Q}$ can be written as

$$-\frac{1}{(E_m - E_n)/kT}[\exp(-E_m/kT) - \exp(-E_n/kT)] = \exp(-E_n/kT)\frac{1-\exp(-x)}{x} \rightarrow \exp(-E_n/kT)\left(1 - \frac{x}{2} + \frac{x^2}{6} - \ldots\right) \quad (4)$$

with

$$x = \frac{E_m - E_n}{kT} \approx \frac{D}{kT} = \frac{1}{T^*} \quad (5)$$

where the differences between the non-degenerate energy levels belonging to the ground multiplet generally are of the order of D. With increasing T (decreasing x), the leading term in the series expansion in eq 4 effectively decouples the states $|n\rangle$ and $|m\rangle$ in the shielding expression, and

$$Q_{mn} \rightarrow \exp(-E_n/kT) \quad \forall \quad m$$

$$\langle S_a S_b\rangle = \frac{\sum_{nm} Q_{nm}\langle n|S_a|m\rangle\langle m|S_b|n\rangle}{\sum_n \exp(-E_n/kT)} \rightarrow \frac{\sum_n \exp(-E_n/kT)\langle n|S_a S_b|n\rangle}{\sum_n \exp(-E_n/kT)} \quad (6)$$

where the resolution of the identity $\sum_m |m\rangle\langle m| = 1$ has been used.[14] In this situation, the magnetic couplings between the states of the ground multiplet have been eliminated, and only the thermal occupations,

$$p_n = \frac{\exp(-E_n/kT)}{\sum_n \exp(-E_n/kT)} \quad (7)$$

remain. The limiting form of eq 6 was derived in ref 10, starting from an ansatz that *a priori* does not accommodate magnetic couplings. Estimated from the leading coupling term in eq 4, the influence of the magnetic couplings remains below 1% and 5% with $x < 0.02$ and $x < 0.1$, respectively, corresponding to $T^* > 50$ and $T^* > 10$, respectively.

Figure 2 illustrates the dependence of the calculated ^{1}H chemical shifts on the inverse temperature for the two present $S = 3/2$ complexes. The shift values at selected temperatures are also listed in Tables 1 and 2. In Figure 2a is shown the importance of the magnetic couplings between the states of the ground multiplet of the HPYBCO complex with a large ZFS, in a temperature scale from 500 K down to the liquid nitrogen temperature. At room temperature, omission of the magnetic couplings leads maximally to the non-negligible 4 ppm change

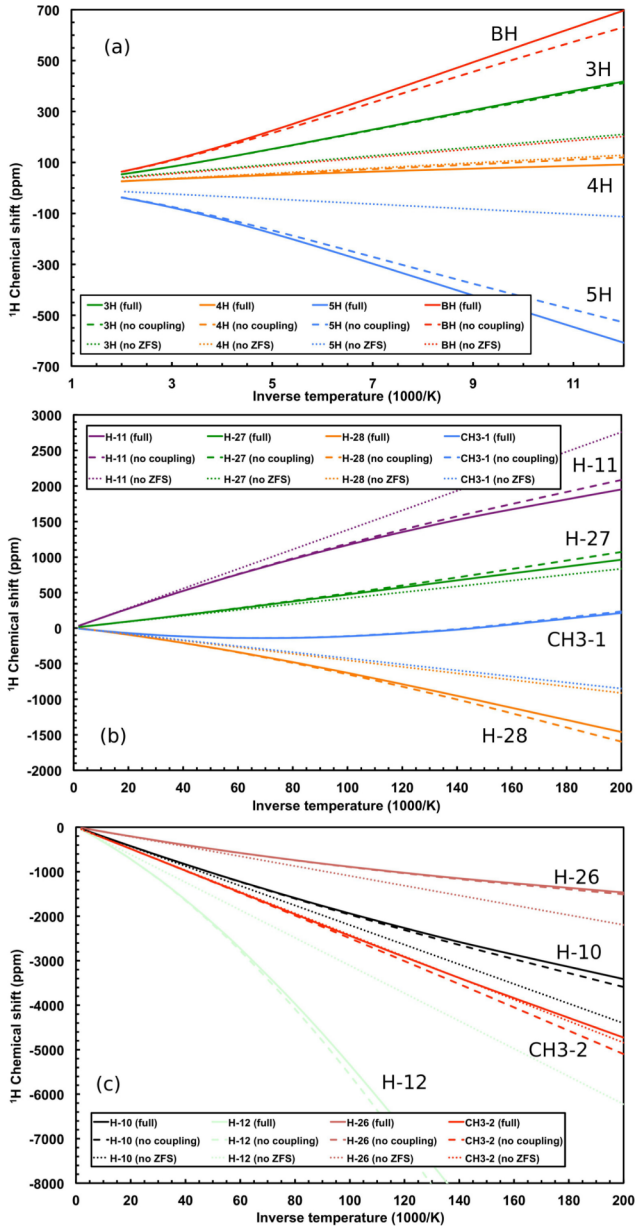

Figure 2. Curie plot of the calculated ^{1}H chemical shifts in (a) a Co(II) complex with a large zero-field splitting (ZFS) and (b,c) a Cr(III) complex with a small ZFS. The full lines correspond to the full SVH expression,[14] including magnetic couplings and thermal occupations of the levels of the ground multiplet. The dashed lines omit magnetic couplings between the non-degenerate states. The dotted lines denote results obtained with the doublet-like formula, in which the ZFS is entirely neglected. All calculations were done at the combined NEVPT2-PBE0/def2-TZVP level as described in the text. The numbering of the nuclei refers to Figure 1. Note the much extended inverse temperature scale in the case of the Cr(III) complex, in panels b and c.

of the chemical shift (of the 5H proton, Table 1). However, larger deviations from the experimental data[24] result at this temperature from the other computational approximations, such as the choice of the DFT functional in the calculations of the $\boldsymbol{A}$-tensors, the deficiencies of the basis sets used, and the neglect of intermolecular interaction effects.[18] Furthermore, limitation to the ZFS Hamiltonian of the form $\boldsymbol{S}\cdot\boldsymbol{D}\cdot\boldsymbol{S}$ may also influence the agreement with experiment, in this case with a

DOI: 10.1021/acs.jctc.5b00656
J. Chem. Theory Comput. 2015, 11, 4840−4849

Table 1. Calculated Chemical Shifts (in ppm) at Various Temperatures with Respect to TMS for Protons in the Cobalt(II) Pyrazolylborate (HPYBCO) Complex Using the Full SVH Theory (Eq 1), Using the Method Omitting Magnetic Coupling Terms (Eq 6), and Omitting Zero-Field Splitting Altogether (Eq 9)[a]

T/K	theory	3H	4H	5H	BH
500	full SVH	53.6	26.0	−38.0	64.0
	no coupling	53.5	26.3	−37.0	63.2
	no zfs	42.2	26.8	−13.7	39.1
400	full SVH	68.1	30.5	−56.2	85.6
	no coupling	67.9	31.1	−54.4	84.2
	no ZFS	50.6	31.9	−18.7	47.2
298	experiment[b]	94.2	42	−111	122.0
	full SVH	95.2	37.9	−92.9	128.3
	no coupling	94.9	39.3	−88.8	125.0
	no ZFS	65.1	40.6	−27.2	61.2
150	full SVH	216.3	61.9	−277.1	334.5
	no coupling	214.4	70.4	−253.3	315.1
	no ZFS	120.8	74.4	−60.0	115.1
75	full SVH	466.9	98.7	−689.0	785.2
	no coupling	459.3	132.8	−593.3	706.9
	no ZFS	233.1	142.5	−126.0	223.7

[a]All calculations at the combined NEVPT2-PBE0/def2-TZVP level as described in the text. The numbering of the nuclei refers to Figure 1. [b]Reference 24. The original experimental assignments[24] of the 3H and 5H signals have been interchanged on the basis of the calculations of ref 18.

relatively strong SO coupling.[12] Finally, fully relativistic calculations of the involved EPR tensors, including also scalar effects, would offer further potential for improvement.[15] At lower temperatures, very substantial deviations from the full SVH theory develop for the Co(II) complex as a result of omitting the couplings. In contrast, the Cr(III) complex with small ZFS (Figure 2b,c) starts to show significant effects of magnetic couplings only at liquid nitrogen temperatures and below. An all-DFT calculation including also the ZFS and *g*-tensors computed at that level was seen in ref 18 to lead to ^{1}H chemical shifts with little resemblance to the experimental data in the case of large-ZFS Co(II) systems. However, the DFT data at the "no coupling" level computed in ref 46 for the present small-ZFS Cr(III) system correlate qualitatively well with the experiment, although the present calculations still represent an improvement.

The Curie plots of the computed isotropic ^{13}C chemical shifts in the two S = 1 metallocenes, nickelocene and chromocene, are given in Figure S1 in the SI. Figure S2 illustrates, in turn, the ^{13}C nuclear shielding anisotropy in the $NiCp_2$ system. The corresponding numerical data at selected temperatures, including also the ^{1}H shifts and $\Delta\sigma(^{1}H)$ in $NiCp_2$, are given in Table S4. The findings for these two systems roughly correspond to those for the S = 3/2 cases; for the $NiCp_2$ complex with the larger ZFS among the two systems, deviations due to omitting the magnetic couplings amount to about 1 ppm at room temperature, whereas the corresponding effects of the couplings are negligible for $CrCp_2$. A satisfactory overall agreement with experiment is obtained for the calculated data at both the full SVH and "no coupling" levels.

The contributions of the physical mechanisms to the isotropic ^{1}H shielding constant for the two S = 3/2 systems, according to the term breakdown of refs 10 and 18, are shown in Tables S5 and S6. On going from the full SVH formula to omitting the magnetic couplings, the results for the Co(II) system change in a qualitatively modest but quantitatively non-negligible way at room temperature (Table S5). In particular, the relative proportions of the terms remain intact. The very large σ_{dip} contribution, which arises entirely due to ZFS,[10] is

Table 2. As Table 1, but for Quinolyl-Functionalized Cyclopentadienyl Cr(III) Complex

T/K	theory	H-10	H-11	H-12	H-26	H-27	H-28	CH_3-1	CH_3-2
500	full SVH	−35.4	35.1	−54.6	−13.6	16.4	−1.1	−6.4	−46.4
	no coupling	−35.4	35.1	−54.6	−13.6	16.4	−1.1	−6.4	−46.4
	no ZFS	−35.5	35.2	−53.5	−13.7	16.4	−1.1	−6.5	−46.3
400	full SVH	−46.4	42.0	−70.7	−19.1	18.5	−3.5	−8.5	−58.5
	no coupling	−46.4	42.0	−70.7	−19.1	18.5	−3.5	−8.5	−58.5
	no ZFS	−46.5	42.1	−69.1	−19.2	18.5	−3.4	−8.7	−58.5
298	experiment[27]	−56	51.8	−78	−15.8	15.3	—	27.6	−41.1
	DFT[a]	−85.3	66.9	−117.9	−30.9	24.2	−14.6	26.8	−55.8
	full SVH	−65.1	53.6	−98.7	−28.4	22.1	−7.5	−12.0	−79.3
	no coupling	−65.1	53.6	−98.7	−28.4	22.1	−7.5	−11.9	−79.3
	no ZFS	−65.4	53.9	−95.8	−28.6	22.0	−7.3	−12.3	−79.2
150	full SVH	−137.4	98.5	−210.4	−64.2	36.0	−23.5	−25.0	−159.7
	no coupling	−137.4	98.5	−210.5	−64.2	36.0	−23.5	−25.0	−159.7
	no ZFS	−138.5	99.4	−199.0	−65.1	35.7	−22.5	−26.4	−159.4
75	full SVH	−281.2	187.3	−452.2	−134.8	64.5	−56.9	−49.0	−322.0
	no coupling	−281.2	187.4	−452.8	−134.8	64.5	−56.9	−49.0	−322.2
	no ZFS	−285.6	191.0	−406.7	−138.5	63.3	−53.2	−54.8	−320.8

[a]Reference 46 DFT (B3LYP) calculation using the "no coupling" level.

DOI: 10.1021/acs.jctc.5b00656
J. Chem. Theory Comput. 2015, 11, 4840−4849

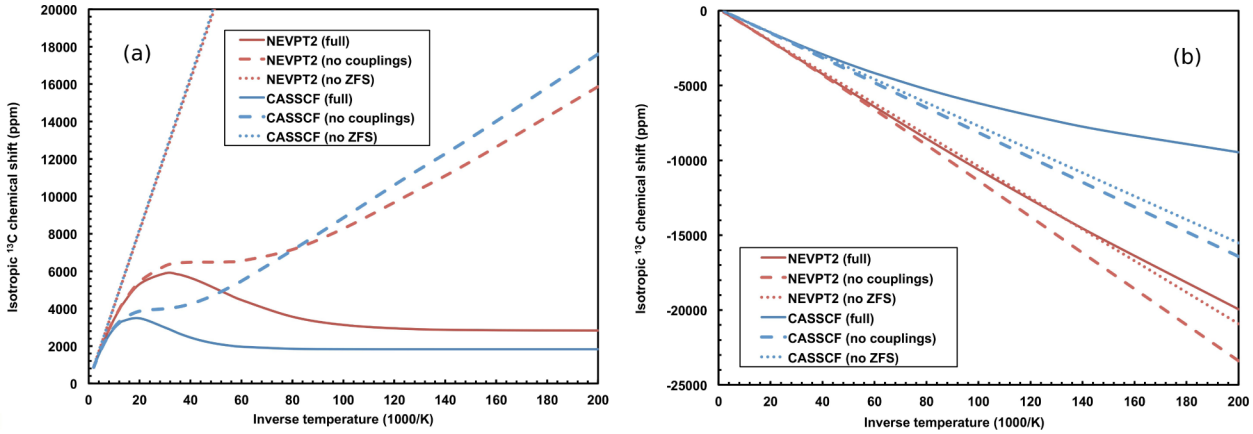

Figure 3. Curie plot of the isotropic ^{13}C chemical shift in spin-1 (a) nickelocene and (b) chromocene in the temperature range from 500 to 5 K. Results using the full SVH theory (eq 1), using the method omitting magnetic coupling terms (eq 6), and omitting zero-field splitting (ZFS) altogether (eq 9). All calculations at the combined NEVPT2-PBE0/def2-TZVP and CASSCF-PBE0/def2-TZVP levels, as described in the text.

reduced from the results of the full theory to the "no coupling" situation. Furthermore, also the contact shielding σ_{con} changes by ca. 1 ppm for each of the four proton signals. For the Cr(III) systems with small ZFS, the physical contributions (Table S6) remain, for all practical purposes, identical at room temperature, as a result of omitting the magnetic couplings.

The corresponding breakdown to the physical shielding contributions at room temperature is given for the ^{13}C and ^{1}H chemical shifts in the metallocenes, as well as $\Delta\sigma(^{13}C)$ in $NiCp_2$, in Table S7. For $NiCp_2$, which has a relatively large D parameter of ZFS, significant effects amounting to 3, 4.5, and 0.6 ppm for $\delta(^{13}C)$, $\Delta\sigma(^{13}C)$, and $\delta(^{1}H)$, respectively, result in the contact contribution σ_{con} from omitting the magnetic coupling effects. This term is, notably, non-vanishing also for the shielding anisotropy in the presence of ZFS. For $CrCp_2$, the omission of the magnetic couplings does not change the shielding contributions to an appreciable extent at 298 K.

4.2. Doublet-like Theory. Upon further increasing the effective temperature, assuming that the excited multiplets nevertheless remain negligibly occupied, ZFS within the ground multiplet can be omitted altogether. In this situation, all the states of the multiplet will be equally occupied, $p_n \to 1/(2S+1)$, and[13]

$$\frac{\sum_n \exp(-E_n/kT)\langle n|S_aS_b|n\rangle}{\sum_n \exp(-E_n/kT)} \to \frac{\sum_n \langle n|S_aS_b|n\rangle}{2S+1} = \frac{\mathrm{Tr}S_aS_b}{2S+1} = \frac{S(S+1)}{3}\delta_{ab} \quad (8)$$

Hence, neglecting not only the magnetic couplings but also the differing thermal occupations of the levels of the ground multiplet returns the "doublet-like" shielding formula,[9,14,16,22]

$$\sigma_{K,\epsilon\tau} = \sigma^{orb}_{K,\epsilon\tau} - \frac{\mu_B}{\gamma_K \hbar kT}\frac{S(S+1)}{3}\sum_a g_{\epsilon a}A_{K,a\tau} \quad (9)$$

which does not require the computation of ZFS. This result is (naturally) exact in the $S = {}^1/_2$ case, and it also is commonly used in approximate treatments of systems with $S \geq 1$.

Figures 2, S1, and S2 illustrate the quality of this approximation, omitting ZFS altogether, for ^{1}H shifts in the present $S = 3/2$ systems, ^{13}C shifts in the $S = 1$ metallocenes, and the ^{13}C shielding anisotropy in $NiCp_2$, respectively. Numerical data at selected temperatures (also for the ^{1}H shifts of both metallocenes and the ^{1}H shielding anisotropy in $NiCp_2$) are listed in Tables 1 [Co(II) system HPYBCO], 2 [Cr(III) complex], and S4 (metallocenes). At this "no ZFS" level, the Curie plots remain linear throughout the temperature range, as the only source of non-Curie behavior would arise from the presently excluded excited multiplets in the doublet-like theory. Omitting ZFS is seen to result in a gross deviation from the SVH theory for the cases with large ZFS, the ^{1}H shift in the Co(II) system HPYBCO (Figure 2a) and both ^{13}C and ^{1}H shielding parameters in $NiCp_2$ (Figures S1 and S2 and Table S4), at the experimentally relevant temperatures. In contrast, the effects of even this approximation remain smaller than the inaccuracies resulting from the choices (*vide supra*) in the present electronic structure calculations down to 150 K in the small-ZFS Cr(III) and Cr(II) complexes (Figure 2b,c and Table S4). Hence, omitting ZFS altogether may be a well-motivated option, particularly as its accurate calculation represents a significant methodological challenge, in some $S \geq 1$ cases.

Investigation of the physical contributions to the shielding parameters at T = 298 K (Tables S5–S7) reveals two characteristic features in the hierarchy of the present three levels of approximation. The usually dominant isotropic shielding term, σ_{con}, remains the same in both the cases of omitting the ZFS entirely and only omitting the magnetic couplings. This is due to the fact that $\mathrm{Tr}\langle \boldsymbol{SS}\rangle = S(S+1)$ at both these levels. In contrast, in the full SVH theory this equality no longer holds, and the value of $S(S+1)$ is reached only at the high-T* limit. Second, when ZFS is neglected entirely, several contributions to both the isotropic shielding constant σ and the rank-2 shielding anisotropy $\Delta\sigma$ vanish by symmetry, as seen in Table S1. In the case of the rank-0 isotropic shielding constant σ, the vanishing contributions are the dipolar terms σ_{dip}, $\sigma_{dip,2}$, and $\sigma_{dip,3}$, as well as the "anisotropic contact" term $\sigma_{c,aniso}$. For the rank-2 anisotropy $\Delta\sigma$, the vanishing terms are, correspondingly, the contact terms σ_{con}, $\sigma_{con,2}$, and $\sigma_{con,3}$, as well as the "antisymmetric" term σ_{as}. The symmetry-based vanishing of all these terms is numerically significant for the observable chemical shift and shielding anisotropy only in the cases with large ZFS, presently HPYBCO and $NiCp_2$, whereas these terms are of no concern for the two Cr complexes at room temperature. In the case of the HPYBCO complex, the isotropic part of the pseudocontact shielding, σ_{pc}, undergoes a significant reduction in absolute magnitude from the "no

DOI: 10.1021/acs.jctc.5b00656
J. Chem. Theory Comput. 2015, 11, 4840−4849

coupling" to the "no ZFS" level (Table S5), whereas no such dramatic change can be seen for $NiCp_2$ (Table S7).

5. $S = 1$ METALLOCENES AT LOW TEMPERATURE

Figure 3 illustrates the inverse temperature dependence of the ^{13}C chemical shift in the two $S = 1$ metallocenes, this time in the full temperature scale from 500 to 5 K. In the case of $NiCp_2$, the full SVH theory results in the notable, non-monotonic Curie plot, with shift maximum at around $T = 50$ and 30 K in the present CASSCF and NEVPT2 calculations, respectively. The non-monotonic behavior was predicted recently in ref 16. In contrast, $CrCp_2$ does not feature such a feature at our best, NEVPT2 computational level. The essential difference between the two systems is, as noted above, the sign of the D parameter of ZFS: positive in $NiCp_2$ and negative as well as smaller in $CrCp_2$.

We note in passing that an entirely wrong temperature dependence at low temperatures follows from using the doublet-like formula (the "no ZFS" approximation), devoid of any non-linearity in the Curie plot. It was formally shown in ref 14 that the "no coupling" approximation fails, too, at low temperatures, as evident for both $NiCp_2$ and $CrCp_2$ (Figure 3).

5.1. Magnetic Couplings at Low Temperature. For an axial integer-spin system, the energy levels corresponding to the ZFS Hamiltonian of the form $\boldsymbol{S}\cdot\boldsymbol{D}\cdot\boldsymbol{S}$ are arranged in one singly degenerate state and doubly degenerate pairs of states. In the axial (almost axial, in the case of $CrCp_2$) $S = 1$ metallocenes, when $D > 0$, the singly degenerate state is the ground state, and the two remaining, excited states of the ground multiplet are at relative energy D with respect to the ground state. The opposite situation prevails for systems with $D < 0$, where the ground state is doubly degenerate. The extremum of the chemical shift in axial, integer-spin systems is related to the higher degeneracy of the excited level(s) than that of the ground state. As evident from the above, at high temperature the characteristic temperature dependence of the pNMR shielding arises from the Curie-like $1/kT$ prefactor of the hyperfine shielding term (eq 1), due to the facts that, first, the magnetic coupling terms become unimportant and, eventually, the entire ZFS can be omitted. At low temperatures, however, ZFS and magnetic couplings between the sub-states of the ground multiplet are indispensable. In particular, the chemical shifts in the axial $S = 1$ $NiCp_2$ system with a singly degenerate ground state converge to temperature-independent values.[14,16] This indicates that the influence of the Curie prefactor $1/kT$ is entirely canceled at low temperature, in contrast to the $CrCp_2$ system (Figure 3b), with a doubly degenerate ground state.

Aligning the zero of the energy scale with the ground-state energy in the low-temperature limit, the diagonal ($E_m = E_n$) blocks of the Kurland–McGarvey $\boldsymbol{Q}$ matrix, corresponding to the degenerate sets of states, become

$$\exp(-E_n/kT) \rightarrow \begin{cases} 1 & \text{for } n = 0 \text{ (the ground state)} \\ 0 & \text{for all the excited states} \end{cases} \tag{10}$$

The Boltzmann factors $\exp(-E_n/kT)$ approach unity for the ground state(s) and zero for (all) the excited state(s), to reflect the negligible thermal occupation of the latter at low enough temperatures. On the other hand, the components in the off-diagonal coupling blocks (for $E_m \neq E_n$) of $\boldsymbol{Q}$ become

$$-\frac{kT}{E_m - E_n}[\exp(-E_m/kT) - \exp(-E_n/kT)] \rightarrow \begin{cases} \dfrac{kT}{E_{\text{exc}}} & \text{when } m \text{ or } n = 0 \\ 0 & \text{otherwise} \end{cases} \tag{11}$$

The components Q_{mn}, for which one of the states m,n does or does not belong to the singly or doubly degenerate ground state of the $\boldsymbol{S}\cdot\boldsymbol{D}\cdot\boldsymbol{S}$ Hamiltonian, are different. Here, E_{exc} is the excitation energy, equal to $|D|$ for axial $S = 1$ systems.

For the two axial $S = 1$ metallocenes, $NiCp_2$ and $CrCp_2$ with positive and negative D, respectively, the $\boldsymbol{Q}$ matrix takes the following forms:

$$\boldsymbol{Q} = \begin{pmatrix} 0 & 0 & \dfrac{kT}{D} \\ 0 & 0 & \dfrac{kT}{D} \\ \dfrac{kT}{D} & \dfrac{kT}{D} & 1 \end{pmatrix} \quad (D > 0)$$

$$\boldsymbol{Q} = \begin{pmatrix} 0 & \dfrac{kT}{D} & \dfrac{kT}{D} \\ \dfrac{kT}{D} & 1 & 1 \\ \dfrac{kT}{D} & 1 & 1 \end{pmatrix} \quad (D < 0) \tag{12}$$

where the bottom row always corresponds to the ground state. Using the matrix of the $D > 0$ case and the eigenstates $|n\rangle$ of $\boldsymbol{S}\cdot\boldsymbol{D}\cdot\boldsymbol{S}$ in the nominator of the expression of the diagonal elements $\langle S_a S_a\rangle$ of the SVH shielding formula (eq 2) leads to

$$\sum_{nm} Q_{nm}\langle n|\begin{pmatrix} S_x \\ S_y \\ S_z \end{pmatrix}|m\rangle\langle m|\begin{pmatrix} S_x \\ S_y \\ S_z \end{pmatrix}|n\rangle = \begin{pmatrix} \dfrac{2kT}{D} \\ \dfrac{2kT}{D} \\ 0 \end{pmatrix} \quad (D > 0) \tag{13}$$

where the molecular axis is along the z-coordinate. The following combination

$$\frac{1}{3}\sum_{nm} Q_{nm}\mathrm{Tr}\langle n|\boldsymbol{S}|m\rangle\langle n|\boldsymbol{S}|m\rangle = \frac{4}{3}\frac{kT}{D} \quad (D > 0) \tag{14}$$

contributes to the isotropic shielding constant. The proportionality of eq 14 to kT cancels exactly with the Curie prefactor $1/kT$ in the hyperfine shielding formula (eq 1), and the shielding constant (as well as the anisotropy with respect to the direction of the molecular axis) acquires a constant low-temperature value, in the case of a non-degenerate ground state. This result was obtained earlier using a different argument in ref 14. The different temperature dependences at the high-T and low-T limits, $1/kT$ and constant, respectively, imply the possibility of an extremum occurring in the isotropic shielding constant or chemical shift, as observed for $NiCp_2$ (Figure 3a).

In the $D < 0$ case and, hence, the doubly degenerate ground state, the appropriate $\boldsymbol{Q}$ from eq 12 gives

DOI: 10.1021/acs.jctc.5b00656
J. Chem. Theory Comput. 2015, 11, 4840–4849

$$\sum_{nm} Q_{nm}\langle n|\begin{pmatrix}S_x\\S_y\\S_z\end{pmatrix}|m\rangle\langle m|\begin{pmatrix}S_x\\S_y\\S_z\end{pmatrix}|n\rangle = \begin{pmatrix}1+\frac{kT}{D}\\1+\frac{kT}{D}\\1\end{pmatrix} \quad (D<0) \tag{15}$$

and

$$\frac{1}{3}\sum_{nm} Q_{nm}\mathrm{Tr}\langle n|\boldsymbol{S}|m\rangle\langle n|\boldsymbol{S}|m\rangle = 1+\frac{2}{3}\frac{kT}{D} \quad (D<0) \tag{16}$$

The presence of the leading, constant term in eq 16 indicates that the inverse Curie temperature dependence of the prefactor is not canceled in the case of a doubly degenerate ground state, implying that no extremum of the chemical shift may be expected for $CrCp_2$ (Figure 3b).

5.2. Chemical Shift Extremum. The existence of the chemical shift extremum can be ascertained by writing out the analytical expression of the isotropic shielding constant according to the Kurland–McGarvey (or SVH) theory in the case of an axial $S = 1$ system. Related formulas for this and other cases were recently given in ref 16. In this case we assume that the D- and g-tensors have a common principal axis system, with the unique principal axis for both tensors coinciding with the molecular z axis: $\boldsymbol{D} = \mathrm{Diag}(0, 0, D)$ and $\boldsymbol{g} = \mathrm{Diag}(g_\perp, g_\perp, g_\parallel)$, whereas the HFC tensor of the nucleus K in a general, off-axis position, has the form

$$\boldsymbol{A}_K = \begin{pmatrix}A_{K,xx} & A_{K,xy} & A_{K,xz}\\A_{K,yx} & A_{K,yy} & A_{K,yz}\\A_{K,zx} & A_{K,zy} & A_{K,zz}\end{pmatrix} \tag{17}$$

which in general contains an antisymmetric contribution (implying $A_{\epsilon\tau} \neq A_{\tau\epsilon}$) due to the SO interaction. Equation 1 leads to the following expression for the isotropic hyperfine shielding constant in this case:

$$\sigma_K^p = -\frac{2}{3}\frac{\mu_B}{\gamma_K \hbar kT} \times \frac{A_{K,zz}g_\parallel + \frac{kT}{D}[\exp(D/kT) - 1](A_{K,xx} + A_{K,yy})g_\perp}{\exp(D/kT) + 2} \tag{18}$$

The temperature derivative $d\sigma^p{}_K/dT$ equals zero, indicating an extremum, at the root of the following equation:

$$2kTA_{K,zz}g_\parallel + \exp(D/kT)[(kT - D)A_{zz}g_\parallel + 3kT(A_{K,xx} + A_{K,yy})g_\perp] = 0 \tag{19}$$

A numerical solution of eq 19 can be found for the two present metallocenes, with different values of D, using $g_\perp$ and $g_\parallel$ listed in Table S3 (NEVPT2/def2-TZVP results used here), as well as, for ^{13}C, the A_C-tensors (at the PBE0/def2-TZVP level) listed in Table S8. Figure 4 illustrates the results. The temperatures T_m of shift extrema are found to be simply related to the value of D, $T_m = cD$, where the linear coefficient of proportionality c equals 0.8351 K/cm^{-1} for $NiCp_2$ and 0.3658 K/cm^{-1} for $CrCp_2$. It is notable that the existence of a physically meaningful, *positive* T_m requires $D > 0$. For the actual values appropriate for the two metallocenes, $D = 40.1$ cm^{-1} for $NiCp_2$ and -10.1 cm^{-1} for $CrCp_2$, values of T_m are obtained as 33.4 and -4.12 K. Indeed, a shift maximum is seen in the NEVPT2 data of $NiCp_2$ (Figure 3a) at the correct temperature, whereas no extremum is seen for $CrCp_2$.

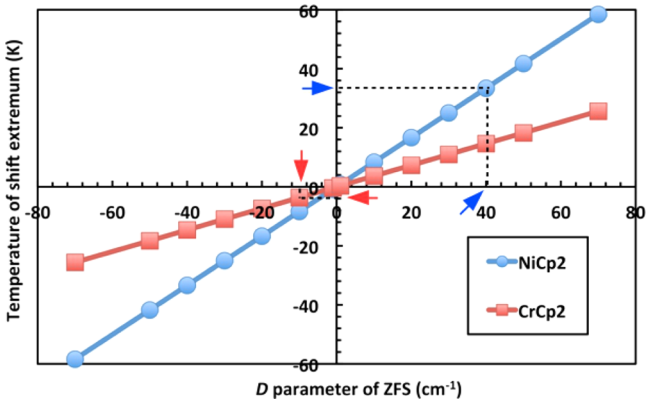

Figure 4. Temperature of the ^{13}C chemical shift extremum as a function of the magnitude of the D parameter of zero-field splitting in axial $S = 1$ metallocenes. Results with calculated $\boldsymbol{g}$ and $\boldsymbol{A}$ as appropriate to $NiCp_2$ and $CrCp_2$ are given. The values obtained for the actual value of D in the two systems at the NEVPT2/def2-TZVP level are highlighted.

It would be interesting to verify the non-monotonic behavior of the chemical shift experimentally; e.g., the measured $D = 25.6$ cm^{-1} (ref 30) suggests that the measurements on $NiCp_2$ would have to be extended to a very low temperature, about 20 K. Qualitatively similar arguments lead to the existence of a chemical shift extremum in axial systems of also higher than triplet multiplicity, provided that $D > 0$.

6. CONCLUSIONS

We have analyzed the Kurland–McGarvey nuclear shielding theory for paramagnetic systems, and particularly its special case limited to the zero-field-split ground multiplet, parametrized by the EPR Hamiltonian. The correct shielding expression for this situation was recently provided by Soncini and Van den Heuvel. Two physical features are characteristic of the theory: (1) thermal occupations of the substates and (2) magnetic couplings between them via the Zeeman and hyperfine interactions. These are reflected in the Kurland–McGarvey coupling matrix $\boldsymbol{Q}$ as the diagonal and off-diagonal blocks, containing the Boltzmann factors for the matrix components Q_{nm} corresponding to pairs of states n, m that are degenerate at the limit of a vanishing magnetic field, and factors depending on the Boltzmann factors and energy differences of pairs of non-degenerate states, respectively. At sufficiently high temperatures, depending on the magnitude of the ZFS specific to the system in question, the off-diagonal blocks in $\boldsymbol{Q}$ acquire an uncoupled form, rendering the shielding tensor expression to contain a product of the Zeeman and hyperfine interactions, which is effectively thermally averaged in the available substates. At still higher temperatures, provided that the excited multiplets nevertheless remain unoccupied, all the substates of the ground multiplet become effectively degenerate, with equal occupation probability. In this situation one can omit the ZFS altogether, with significant computational savings. These features were demonstrated on two $S = 3/2$ complexes with large and small D parameters of the ZFS.

DOI: 10.1021/acs.jctc.5b00656
J. Chem. Theory Comput. 2015, 11, 4840–4849

As shown by others, at low temperatures the use of the full theory with both thermal occupations and magnetic couplings is essential for determing the correct temperature dependence of the shielding parameters. In particular, the recently found occurrence of the chemical shift extremum for nickelocene, an axial $S = 1$ system, was analyzed by taking the low-temperature limit of the $\mathbf{Q}$ matrix. It was shown that, for this integer-spin system, the existence of the extremal value is associated with a positive D parameter, which implies that the ground state of the triplet manifold is non-degenerate and the excited state is doubly degenerate. In this case, the temperature dependence of the $1/kT$ Curie-type prefactor of the hyperfine shielding contribution is exactly canceled by the limiting form of the coupling terms in the $\mathbf{Q}$-matrix, proportional to kT. The differing high- and low-temperature limiting behaviors imply the possibility of an extremum at intermediate temperatures, and analytical differentiation of the shielding expression of the Kurland−McGarvey theory with respect to the temperature reveals that such an extremum occurs at physically meaningful, positive temperatures only when $D > 0$. Therefore, chromocene with a negative D parameter does not feature such an extremum.

■ ASSOCIATED CONTENT

Supporting Information

The Supporting Information is available free of charge on the ACS Publications website at DOI: 10.1021/acs.jctc.5b00656.

Recapitulation of the Kurland−McGarvey shielding theory and the case of zero-field split ground multiplet; table of the tensorial symmetry properties of the various physical contributions to the paramagnetic nuclear shielding tensor; Curie plots of the isotropic ^{13}C chemical shifts in $NiCp_2$ and $CrCp_2$ from 500 K down to liquid nitrogen temperatures, as well as that of the ^{13}C shielding anisotropy in $NiCp_2$; optimized geometry of the quinolyl-functionalized cyclopentadienyl Cr(III) complex; table of the computed parameters of the g- and $\boldsymbol{D}$-tensors in the investigated complexes; tables of the physical contributions to the proton shielding constants in the $S = 3/2$ Co(II) and Cr(III) complexes, as well as the proton and carbon-13 shielding parameters in $NiCp_2$ and $CrCp_2$, according to the full SVH theory, omitting the magnetic couplings, and omitting ZFS altogether, at 298 K; calculated components of the ^{13}C HFC tensor in the two metallocenes (PDF)

■ AUTHOR INFORMATION

Corresponding Author

*E-mail: juha.vaara@iki.fi.

Notes

The authors declare no competing financial interest.

■ ACKNOWLEDGMENTS

Mr. Jyrki Rantaharju (Oulu) is thanked for useful advice with the MATHEMATICA software. The research leading to these results has received funding from the People Programme (Marie Curie Actions) of the European Union's Seventh Framework Programme FP7/2007-2013 under REA grant agreement no. 317127. Computational resources were partially provided by CSC-IT Center for Science (Espoo, Finland) and the Finnish Grid Initiative project. The work of J.V. and J.M. was additionally supported by the directed programme in Computational Science of the Academy of Finland.

■ REFERENCES

(1) Bertini, I.; Luchinat, C.; Parigi, G. *Solution NMR of Paramagnetic Molecules*; Elsevier: Amsterdam, 2001.
(2) Grey, C. P.; Dupré, N. *Chem. Rev.* **2004**, *104*, 4493.
(3) Kaupp, M.; Köhler, F. H. *Coord. Chem. Rev.* **2009**, *253*, 2376.
(4) Keizers, P. H. J.; Ubbink, M. *Prog. Nucl. Magn. Reson. Spectrosc.* **2011**, *58*, 88.
(5) *Calculation of NMR and EPR Parameters: Theory and Applications*; Kaupp, M., Bühl, M., Malkin, V. G., Eds.; Wiley-VCH: Weinheim, 2004.
(6) Vaara, J. In *High Resolution NMR Spectroscopy*; Contreras, R. H., Ed.; Elsevier: Amsterdam, 2013.
(7) Kurland, R. J.; McGarvey, B. R. *J. Magn. Reson.* **1970**, *2*, 286.
(8) Harriman, J. E. *Theoretical Foundations of the Electron Spin Resonance*; Academic Press: New York, 1978.
(9) Moon, S.; Patchkovskii, S., in ref 5.
(10) Pennanen, T. O.; Vaara, J. *Phys. Rev. Lett.* **2008**, *100*, 133002.
(11) Autschbach, J.; Patchkovskii, S.; Pritchard, B. *J. Chem. Theory Comput.* **2011**, *7*, 2175.
(12) Van den Heuvel, W.; Soncini, A. *Phys. Rev. Lett.* **2012**, *109*, 073001.
(13) Van den Heuvel, W.; Soncini, A. *J. Chem. Phys.* **2013**, *138*, 054113.
(14) Soncini, A.; Van den Heuvel, W. *J. Chem. Phys.* **2013**, *138*, 021103.
(15) Komorovsky, S.; Repisky, M.; Ruud, K.; Malkina, O. L.; Malkin, V. G. *J. Phys. Chem. A* **2013**, *117*, 14209.
(16) Martin, B.; Autschbach, J. *J. Chem. Phys.* **2015**, *142*, 054108.
(17) Gendron, F.; Sharkas, K.; Autschbach, J. *J. Phys. Chem. Lett.* **2015**, *6*, 2183.
(18) Rouf, S. A.; Mareš, J.; Vaara, J. *J. Chem. Theory Comput.* **2015**, *11*, 1683.
(19) Schmitt, S.; Jost, P.; van Wüllen, C. *J. Chem. Phys.* **2011**, *134*, 194113.
(20) Kubica, A.; Kowalewski, J.; Kruk, D.; Odelius, M. *J. Chem. Phys.* **2013**, *138*, 064304.
(21) Ramsey, N. F. *Phys. Rev.* **1950**, *78*, 699.
(22) Pennanen, T. O.; Vaara, J. *J. Chem. Phys.* **2005**, *123*, 174102.
(23) Allen, F. H. *Acta Crystallogr., Sect. B: Struct. Sci.* **2002**, *58*, 380.
(24) Długopolska, K.; Ruman, T.; Danilczuk, M.; Pogocki, D. *Appl. Magn. Reson.* **2009**, *35*, 271.
(25) Angeli, C.; Cimiraglia, R.; Evangelisti, S.; Leininger, T.; Malrieu, J. P. *J. Chem. Phys.* **2001**, *114*, 10252;Angeli, C.; Cimiraglia, R.; Malrieu, J. P. *Chem. Phys. Lett.* **2001**, *350*, 297;Angeli, C.; Cimiraglia, R.; Malrieu, J. P. *J. Chem. Phys.* **2002**, *117*, 9138;Angeli, C.; Borini, S.; Cimiraglia, R. *Theor. Chem. Acc.* **2004**, *111*, 352.
(26) Weigend, F.; Ahlrichs, R. *Phys. Chem. Chem. Phys.* **2005**, *7*, 3297; **2006**, *8*, 1057.
(27) Fernández, P.; Pritzkow, H.; Carbó, J. J.; Hofmann, P.; Enders, M. *Organometallics* **2007**, *26*, 4402.
(28) Hrobárik, P.; Reviakine, R.; Arbuznikov, A. V.; Malkina, O. L.; Malkin, V. G.; Köhler, F. H.; Kaupp, M. *J. Chem. Phys.* **2007**, *126*, 024107.
(29) Aquino, F.; Pritchard, B.; Autschbach, J. *J. Chem. Theory Comput.* **2012**, *8*, 598.
(30) Prins, R.; van Voorst, J. D. W.; Schinkel, C. J. *Chem. Phys. Lett.* **1967**, *1*, 54.
(31) Zvarykina, A. V.; Karimov, Yu. S.; Leonova, E. V.; Lyubovskii, R. B. *Sov. Phys.-Solid State (Engl. Transl.)* **1970**, *12*, 385.
(32) Baltzer, P.; Furrer, A.; Hulliger, J.; Stebler, A. *Inorg. Chem.* **1988**, *27*, 1543.
(33) Li, S.; Hamrick, Y. M.; Van Zee, R. J.; Weltner, W., Jr. *J. Am. Chem. Soc.* **1992**, *114*, 4433.
(34) König, E.; Schnakig, R.; Kanellakopulos, B.; Klenze, R. *Chem. Phys. Lett.* **1977**, *50*, 439.

DOI: 10.1021/acs.jctc.5b00656
J. Chem. Theory Comput. 2015, 11, 4840−4849

(35) Rettig, M. F.; Drago, R. S. *Chem. Commun.* **1966**, 891; *J. Am. Chem. Soc.* **1969**, *91*, 1361.
(36) Heise, H.; Köhler, F. H.; Xie, X. *J. Magn. Reson.* **2001**, *150*, 198.
(37) Köhler, F. H.; Prößdorf, W. *J. Am. Chem. Soc.* **1978**, *100*, 5970.
(38) Blümel, J.; Herker, M.; Hiller, W.; Köhler, F. H. *Organometallics* **1996**, *15*, 3474.
(39) Hebendanz, N.; Köhler, F. H.; Scherbaum, F.; Schlesinger, B. *Magn. Reson. Chem.* **1989**, *27*, 798.
(40) Lee, C.; Yang, W.; Parr, R. G. *Phys. Rev. B: Condens. Matter Mater. Phys.* **1988**, *37*, 785;Becke, A. D. *J. Chem. Phys.* **1993**, *98*, 5648;Stephens, P. J.; Devlin, F. J.; Ashvar, C. S.; Chabalowski, C. F.; Frisch, M. J. *J. Phys. Chem.* **1994**, *98*, 11623.
(41) *Turbomole*, V6.5; a development of University of Karlsruhe and Forschungszentrum Karlsruhe GmbH, TURBOMOLE GmbH, 1989−2007; available from http://www.turbomole.com.
(42) Neese, F. *Orca*, An ab Initio, Density Functional and Semiempirical Program Package, Version 3.0.1; 2012.
(43) Neese, F. *J. Chem. Phys.* **2003**, *118*, 3939; **2005**, *122*, 034107; **2007**, *127*, 164112.
(44) Frisch, M. J.; Trucks, G. W.; Schlegel, H. B.; Scuseria, G. E.; Robb, M. A.; Cheeseman, J. R.; Scalmani, G.; Barone, V.; Mennucci, B.; Petersson, G. A.; Nakatsuji, H.; Caricato, M.; Li, X.; Hratchian, H. P.; Izmaylov, A. F.; Bloino, J.; Zheng, G.; Sonnenberg, J. L.; Hada, M.; Ehara, M.; Toyota, K.; Fukuda, R.; Hasegawa, J.; Ishida, M.; Nakajima, T.; Honda, Y.; Kitao, O.; Nakai, H.; Vreven, T.; Montgomery, J. A., Jr.; Peralta, J. E.; Ogliaro, F.; Bearpark, M.; Heyd, J. J.; Brothers, E.; Kudin, K. N.; Staroverov, V. N.; Kobayashi, R.; Normand, J.; Raghavachari, K.; Rendell, A.; Burant, J. C.; Iyengar, S. S.; Tomasi, J.; Cossi, M.; Rega, N.; Millam, J. M.; Klene, M.; Knox, J. E.; Cross, J. B.; Bakken, V.; Adamo, C.; Jaramillo, J.; Gomperts, R.; Stratmann, R. E.; Yazyev, O.; Austin, A. J.; Cammi, R.; Pomelli, C.; Ochterski, J. W.; Martin, R. L.; Morokuma, K.; Zakrzewski, V. G.; Voth, G. A.; Salvador, P.; Dannenberg, J. J.; Dapprich, S.; Daniels, A. D.; Farkas, O.; Foresman, J. B.; Ortiz, J. V.; Cioslowski, J.; Fox, D. J. *Gaussian 09*, Revision D.01; Gaussian, Inc.: Wallingford, CT, 2009.
(45) Adamo, C.; Barone, V. *J. Chem. Phys.* **1999**, *110*, 6158.
(46) Liimatainen, H.; Pennanen, T. O.; Vaara, J. *Can. J. Chem.* **2009**, *87*, 954.

DOI: 10.1021/acs.jctc.5b00656
J. Chem. Theory Comput. 2015, 11, 4840−4849